Electrochemical, Spectroelectrochemical, and Comparative Studies of Novel Organic Conjugated Monomers and Polymers Featuring the Redox-Active Unit Tetrathianaphthalene

John C. Forgie,[†] Alexander L. Kanibolotsky,[†] Peter J. Skabara,*[,†] Simon J. Coles,[‡] Michael B. Hursthouse,[‡] Ross W. Harrington,[§] and William Clegg[§]

WestCHEM, Department of Pure and Applied Chemistry, University of Strathclyde, Glasgow G1 1XL, U.K., School of Chemistry, University of Southampton, Highfield, Southampton SO17 1BJ, U.K., and School of Chemistry, Newcastle University, Newcastle upon Tyne NE1 7RU, U.K.

Received January 6, 2009; Revised Manuscript Received February 13, 2009

ABSTRACT: A series of monomers has been synthesized and characterized on the basis of the incorporation of tetrathianaphthalene (**1**) and its saturated (**2**) and open cyclic (**3**) forms as fused side groups onto polythiophene chains. The X-ray crystal structures of compounds **1** and **2** are reported. Tetrathianaphthalene (TTN) is an isomer of tetrathiafulvalene (TTF); however, monomer and polymer versions of **1** do not show any similarity to TTF in cyclic voltammetry (CV) or spectroelectrochemical measurements. CV experiments have shown that **1** and **3** are easier to oxidize than **2**, whereas **1** also has an additional reduction peak, giving it a smaller HOMO−LUMO gap than the other two monomers. All three polymers of **1**−**3** have nearly the same oxidation and reduction potentials as well as band gaps; small variations can be attributed to the differences in the side groups. Spectroelectrochemical measurements revealed that the polymers showed electrochromic behavior; switching times and colorimetry measurements are reported. From this data, all three polymers have a color change of red to yellow with poly(**3**) having the best color contrast and percentage change in absorbance from various switching times.

Introduction

Organic conjugated monomers and polymers have attracted a great deal of attention over the last three decades since the discovery that conductivity could be achieved in p-doped polyacetylene.[1] Since then, these materials have found use in many applications such as electrochromics,[2−5] light emitting diodes,[6−9] field effect transistors,[10−13] photovoltaics,[14−17] and sensors.[18−21] Tetrathiafulvalene (TTF) is one of the most studied electroactive materials and is well known for its easily accessed $TTF^{+\bullet}$ and TTF^{2+} oxidation states.[22] TTF and its derivatives have traditionally been used in the creation of superconductors as charge-transfer salts,[23,24] but in recent years, they have also been incorporated into conjugated polymers. Examples include attachment as the side group in polythiophenes.[25−27] Tetrathianaphthalene (TTN), comprising two fused 1,4-dithiin rings, is an isomer of TTF and is often used as a precursor in the synthesis of TTF.[28] To date, there has been no electrochemical analysis on TTN incorporated into conjugated polymers. In this article, we report the synthesis and characterization of three monomers (**1**−**3**) and their electrochemically prepared polymers by electrochemical and spectroelectrochemical experiments. In this comparative study, monomer **1** has a TTN group attached to a terthiophene unit, whereas monomer **2** is the saturated form of **1** and monomer **3** is the open bridge form.

Polymers of these three monomers were grown electrochemically through the polymerization of the terthiophene group. A terthiophene monomer unit was chosen instead of a single thiophene to minimize steric effects and to lower the oxidation potential for electropolymerization.[29,30] In a previous work, it was shown that TTN and 1,4-dithiin rings adopt boat conformations in the neutral state and planar conformations when oxidized.[31−33] Moses et al.[34,35] have shown that TTN can be electrochemically transformed to give TTF through oxidation and then rearrangement. However, Sugimoto et al.[36] have shown that this reaction will not occur if there is extended conjugation; therefore, monomer **1** would be unlikely to take part in any rearrangement reactions when oxidized.

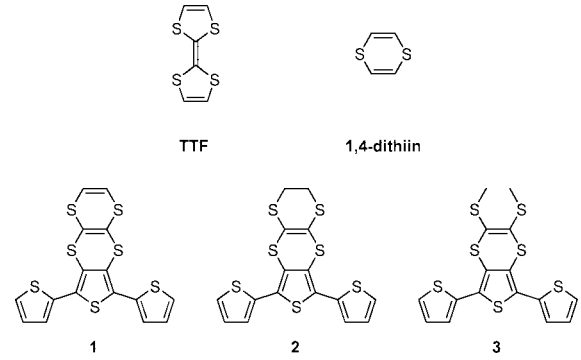

Polythiophene and its variants have good environmental and thermal stability, which has allowed them to be employed in many applications, especially in electrochromics.[37,38] Electrochromic materials have the ability to reversibly change from one state of absorption to another by applying a potential; this effect is caused by modifying the band gap of the material, creating doped states.[39,40] Polythiophene itself is red in the neutral state and blue when doped,[30,37] and through variation of the side group, the three primary colors can be created, thus allowing the development of devices based solely on conjugated polymers.[41,42] In this article, we have investigated the polymers of all three compounds as electrochromic materials by measuring the percentage change in absorbance through different switching times and CIE color coordinates.

Results and Discussion

Synthesis. The synthetic procedures for monomers **1**−**3** are summarized in Scheme 1. Compound **4a**[43] can be easily converted to the carbonyl derivative **4b** in 90% yield using mercury(II) acetate. Cyclization of **4b** with phosphorus penta-

* Corresponding author: peter.skabara@strath.ac.uk.
[†] University of Strathclyde.
[‡] University of Southampton.
[§] Newcastle University.

10.1021/ma900010n CCC: $40.75
Published on Web 03/16/2009

Scheme 1

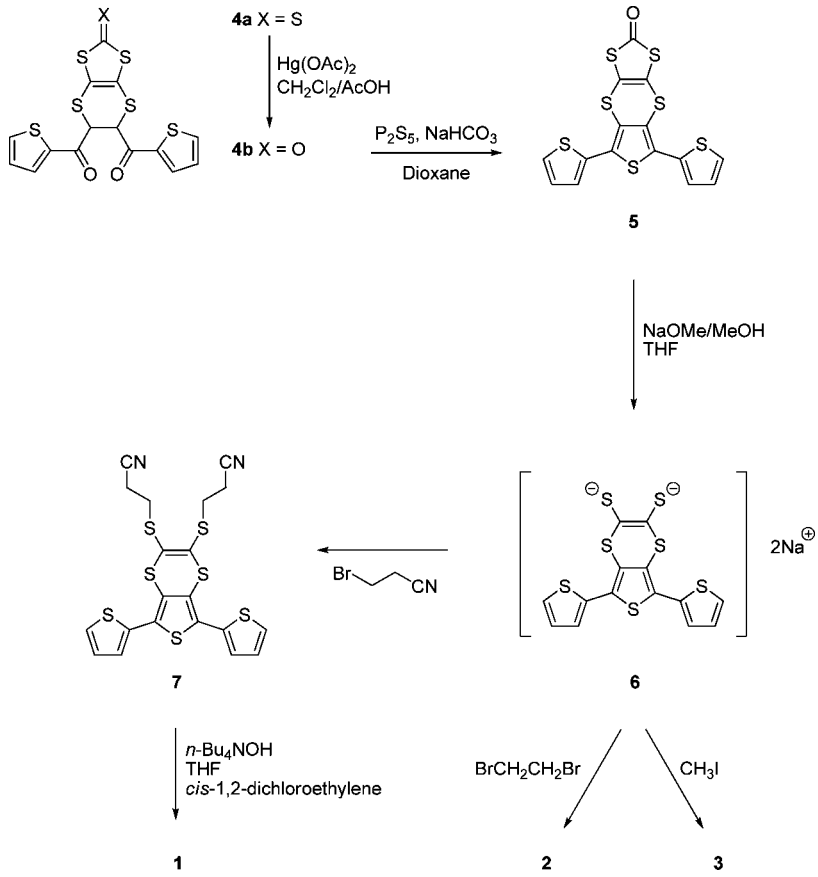

sulfide under basic conditions gave the terthiophene **5** in 84% yield. Generation of the disodium dithiolate reagent **6** in THF solution was accomplished by the addition of freshly prepared sodium methoxide to compound **5**. The subsequent treatment of **6** with 1,2-dibromoethane, methyl iodide, and 3-bromoproprionitrile (in situ) gave compounds **2**, **3**, and **7** in 65, 90, and 79% yields, respectively. The reaction of intermediate **6** with *cis*-1,2-dichloroethylene did not give the desired product when the reaction was carried out at room temperature. It was possible to convert **6** to the product only upon microwave heating, but the reaction did not proceed cleanly and gave a series of byproducts that was difficult to remove from the reaction mixture. It is assumed that the dithiolate acts as a base to convert the dichloro reagent to an acetylenic byproduct by dehydrochlorination. In support of this statement, the reaction of the bis(tetrabutylammonium) analogue of **6**, generated from **7**, with *cis*-1,2-dichloroethylene gave the target compound **1** in 92% yield under mild conditions (room temperature). The bis(tetrabutylammonium) dithiolate can be regarded as a better nucleophile and softer base than intermediate **6**. A complication from the reaction of **6** with *cis*-1,2-dichloroethylene could arise from the possibility of redox chemistry between the dithiolate intermediate and the target compound **1**. An indication of this arises from the electrochemistry of the TTN derivative; CV reveals a reduction peak (−2.03 V), which is absent for **2** and **3**, corresponding to the reduction of the TTN group (vide infra). The more facile reduction of compound **1** in comparison with compound **2** might also be seen in the MS LDI-TOF (−) experiment. (See the Experimental Section.) In the spectrum of **2**, the peak with the largest molecular mass ion corresponds to the deprotonated molecular ion $(M-1)^-$, whereas the molecular ion peak in the spectrum of **1** is exactly M^-. In the course of the investigation, the rearrangement of compound **1** to the TTF analogue was attempted using strong bases such as MeONa and *t*-BuOK. After treating terthiophene **1** with these bases in THF solution (under microwave heating at 120 °C for 30 min), we recovered about half of the starting material along with highly polar side products (tlc evidence). Therefore, we suspect that the reaction of compound **1** under such harsh conditions mostly leads to the decomposition of the starting material by ring opening of the peripheral dithiin unit.

Absorption Spectroscopy and Electrochemistry of Monomers. The electronic absorption spectra for the three monomers in dichloromethane are shown in Figure 1. The absorption maxima are all similar given their near identical structures. Compounds **1** (356 nm), **2** (360 nm), and **3** (362 nm) give expected absorption maxima for the $\pi-\pi^*$ transition of standard terthiophenes with heterocyclic side chains. The onset of the absorption edge gives the HOMO−LUMO gap for the terthiophenes.[44] The values were found to be 2.95 eV for monomer **3** and 2.99 eV for monomers **1** and **2**, indicating that the different side groups had little effect on the $\pi-\pi^*$ transitions.

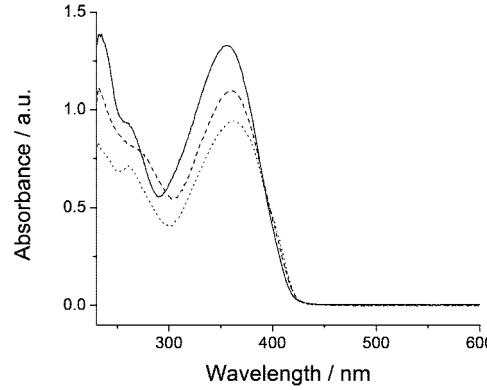

Figure 1. Solution-state electronic absorption spectra for compounds **1** (—), **2** (---), and **3** (•••). Spectra were recorded from solutions in dichloromethane.

Table 1. Electrochemical Data for Compounds 1−3[a]

monomer	E_{1ox} (V)	E_{2ox} (V)	E_{1red} (V)	E_{2red} (V)	HOMO (eV)[b]	LUMO (eV)[b]	E_g (eV)[c]
1	+0.69/+0.66	+0.99[d]	−2.03[d]	−2.28[d]	−5.44	−2.88	2.56
2	+0.75/+0.66	+1.12[d]	−2.27[d]		−5.49	−2.56	2.93
3	+0.68/+0.60	+0.98[d]	−2.30[d]		−5.38	−2.49	2.89

[a] Experimental conditions are the same as those given in Figure 2. [b] HOMO and LUMO values are calculated from the onset of the first peak of the corresponding redox wave and referenced to ferrocene, which has a HOMO of −4.8 eV. [c] E_g is the HOMO−LUMO energy gap. [d] Irreversible peak.

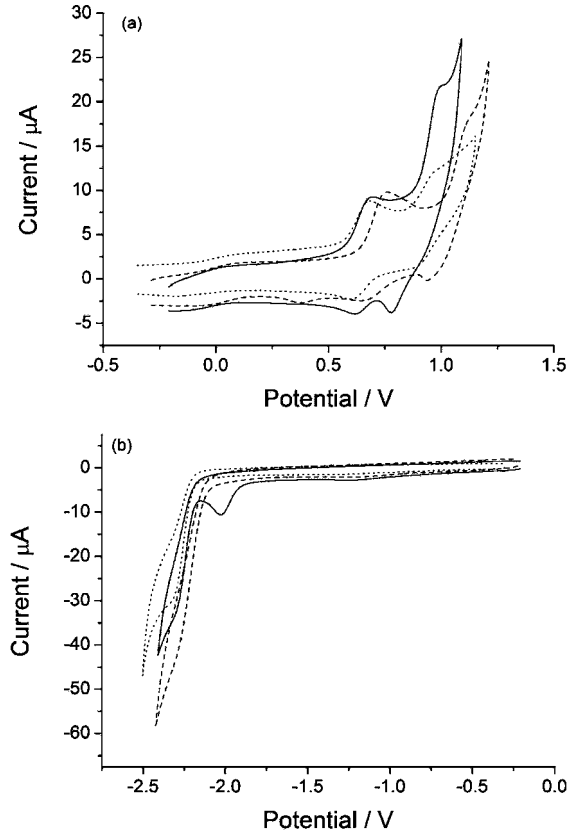

Figure 2. Cyclic voltammograms of (a) oxidation and (b) reduction of **1** (—), **2** (---), and **3** (•••) in CH_2Cl_2 solution (carbon working electrode, silver wire pseudoreference, $(TBA)PF_6$ as the supporting electrolyte (0.1 M), substrate concentration 10^{-4} M, scan rate 100 mV/s). The data are referenced to the Fc/Fc^+ redox couple.

All three monomers have been studied by CV in dichloromethane solution using a silver wire pseudoreference electrode and tetrabutylammonium hexafluorophosphate as the supporting electrolyte. The oxidation of **1**−**3** (Figure 2a) shows one reversible and one irreversible wave in all three cases. The first reversible peak represents a two-electron loss to give a dication species, whereas the second, irreversible peak is a one-electron oxidation. In comparison with TTF, monomer **1** does not show the famous two-wave reversible oxidation to the radical cation and dication. Instead, the results indicate that electrons are removed from the terthiophene component and the TTN unit simultaneously. Despite the similarities of the structures within the series of monomers, the potentials at which the electrons are removed are different (Table 1). Monomers **1** and **3** have a reversible oxidation at $E^1_{1/2}$ = +0.68 V and +0.64 V, respectively, whereas **2** has a higher first oxidation wave at a half-wave potential of +0.71 V. The differences are accounted for by the different side-group structures. Monomer **1** has a lower oxidation potential compared with **2** because there are two additional π electrons and oxidation tends toward an aromatic charged intermediate within two dithiin rings. The lowering of the oxidation potential in **3** is somewhat unexpected and is discussed in more detail below. Similarly, the potential for the second oxidation waves is higher for **2** (+1.12 V) compared with that for **1** (+0.99 V) and **3** (+0.98 V). Irreversible reduction of the monomers (Figure 2b) occurs at −2.28, −2.27, and −2.30 V for **1**, **2**, and **3** respectively. However, compound **1** shows an additional reduction peak (−2.03 V) that corresponds to the irreversible reduction of the TTN group.

The electrochemical HOMO−LUMO gaps of the monomers were calculated from the difference in the onsets of the first oxidation and reduction peaks. Using data referenced to the ferrocene/ferrocenium redox couple, we calculated HOMO and LUMO energies by subtracting the onsets from the HOMO of ferrocene, which has a known value of −4.8 eV. A summary of these data can be seen in Table 1. The HOMO−LUMO gaps are similar for **2** and **3**, with **1** being the smallest. An interesting comparison is the electrochemical value of the HOMO−LUMO gap with respect to the value determined from absorption spectroscopy. For monomers **2** and **3**, the experimental gaps for both techniques are very similar, but for **1**, there is a significant difference (2.99 and 2.56 eV for optical and electrochemical, respectively), suggesting that the TTN side group shows some reductive electroactivity that is independent of the terthiophene chain.

Structural Characterization by X-ray Crystallography and Molecular Modeling. The structure of the TTN derivative (**1**) was determined by single-crystal X-ray diffraction studies using synchrotron radiation. The asymmetric unit consists of two molecules, differing slightly in geometry (conformers A and B, Figure 3). (See the Supporting Information for tables of bond lengths, angles, and experimental data). Of particular note is the fact that the three C−C bonds within the dithiin units of conformer A are 0.03 to 0.08 Å shorter than the corresponding bonds in conformer B. Although these differences are individually marginal (with standard uncertainties of ∼0.02 Å), there is a systematic pattern: comparing analogous C−S bonds between the two conformers reveals that almost all of these bonds are longer in A than in B. (The difference ranges from −0.003 to 0.042 Å). Therefore, conformer B appears to have a more delocalized π-electron distribution. A least-squares fit of the three fused rings of conformers A and B shows a root-mean-square difference of 0.048 Å, with only small differences in the orientations of the terminal thiophene rings relative to this central core.

In general, dithiin rings adopt boat conformations.[33] The degree of bending in the dithiin rings can be expressed as a folding along the S•••S vectors within each ring. The differences between the corresponding folding angles in each conformer of compound **1** are small; the outer dithiin rings have angles of 47.5(4) (S6•••S7) and 46.0(5)° (S13•••S14), whereas the inner rings have values of 52.1(4) (S4•••S5) and 53.7(4)° (S11•••S12). The terthiophene units possess a high degree of coplanarity between adjacent thiophene units, with torsion angles of 179.3(9) (S1−C4−C5−S2), 178.5(9) (S2−C8−C9−S3), 176.0(9) (S8−C20−C21−S9), and 179.9(9)° (S9−C24−C25−S10). In our studies on 3,4-dithio-substituted terthiophenes,[25,45−49] we have found that high degrees of coplanarity within the conjugated chain are formed from an all-anti arrangement of the thiophene rings in which the sulfur atoms of the peripheral rings form close intramolecular S•••S contacts with the 3,4-dithio substituents on the central ring. This is elegantly demonstrated

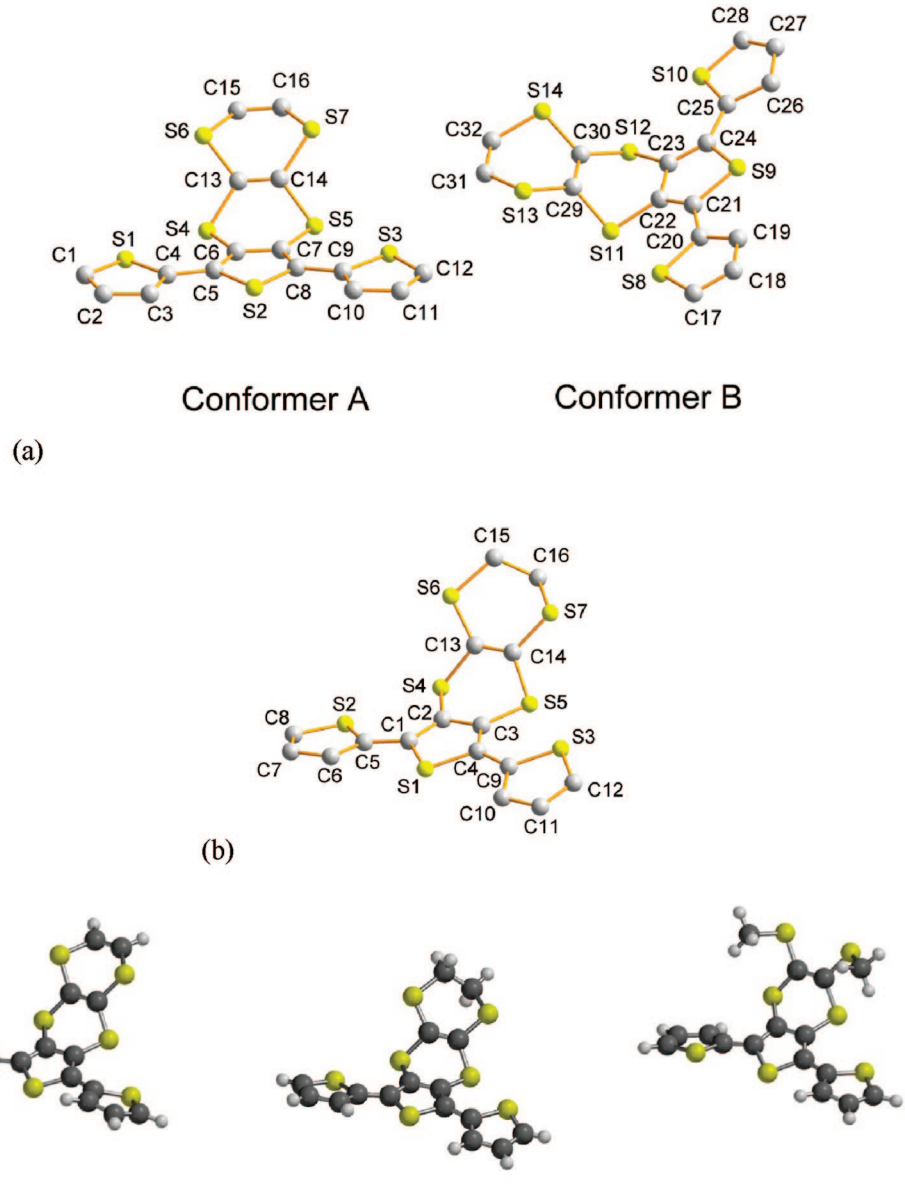

Figure 3. Molecular structures of (a) compound **1** showing the crystallographic asymmetric unit that consists of two conformers and (b) compound **2**. Hydrogen atoms are omitted for clarity. (c) Geometry-optimized structures of compounds **1**−**3** (left to right, respectively). Calculations were performed at the B3LYP/6-31G* level, starting from the observed crystal structures of compounds **1** (for **1** and **3**) and **2**.

in the structure of compound **1**, which has close S···S contacts at distances of 3.182(6) (S1···S4), 3.230(6) (S3···S5), 3.238(6) (S8···S11), and 3.184(7) Å (S10···S12). These values are much smaller than the sum of the van der Waals radii for two sulfur atoms (3.6 Å) and indicate weak bonding between the chalcogens. Finally, one intermolecular short contact exists between the two conformers (S7···S8, 3.506(7) Å; Supporting Information) to link pairs of molecules, but there are no other short intermolecular interactions within the packing diagram.

In compound **2**, the folding vectors are significantly different between the two types of sulfur heterocycles. For the dithiin ring fused to the central thiophene, the value is similar to those in compound **1** (51.6(1)°, S4···S5), whereas the fold in the dihydro−dithiin ring gives a tighter angle (32.5(2)°, S6···S7). Again, the conformation within the terthiophene unit is all-anti. The torsion angles between the thiophenes are 168.0(3) Å (S1−C1−C5−S2) and 175.7 Å (S1−C4−C9−S3), and the S···S contacts between peripheral thiophenes and the 3,4-dithio substituents on the central ring are 3.228(2) (S2···S4) and 3.183(2) Å (S3···S5). The molecules pack with no evidence of $\pi-\pi$ stacking. However, weak intermolecular contacts between S3 and S5 atoms (3.575(2) Å) give rise to a remarkable packing motif, in which groups of six molecules are held together, almost in a spherical arrangement, to give clusters with a diameter of ca. 2.2 nm. (See the Supporting Information.)

To assign the redox processes taking place within the series of terthiophenes, computational calculations were performed using density functional theory at the B3LYP/6-31G* level (Spartan '06). Compound **1** was considered from the initial geometry of its crystal structure (conformer A), as was the case for compound **2**. Calculations performed on terthiophene **3** were based on the crystal structure of **1** with SCH_3 groups substituting the vinylene bridge, followed by relaxation to an equilibrium geometry. In almost all cases, the thiophene units retain anti conformations, apart from one peripheral thiophene in **3**. Compared with the crystal structures of compounds **1** and **2**, planarity is lost in the relaxed structures with torsion angles in the range ca. 20−35°. The calculations were performed for molecules in the gas phase, and it can be assumed that crystal packing forces will have a significant effect on the geometry of the molecule. The folding vectors observed in the dithiin rings of **1** and **2** are in the range 48.2−53.2°, whereas that of the

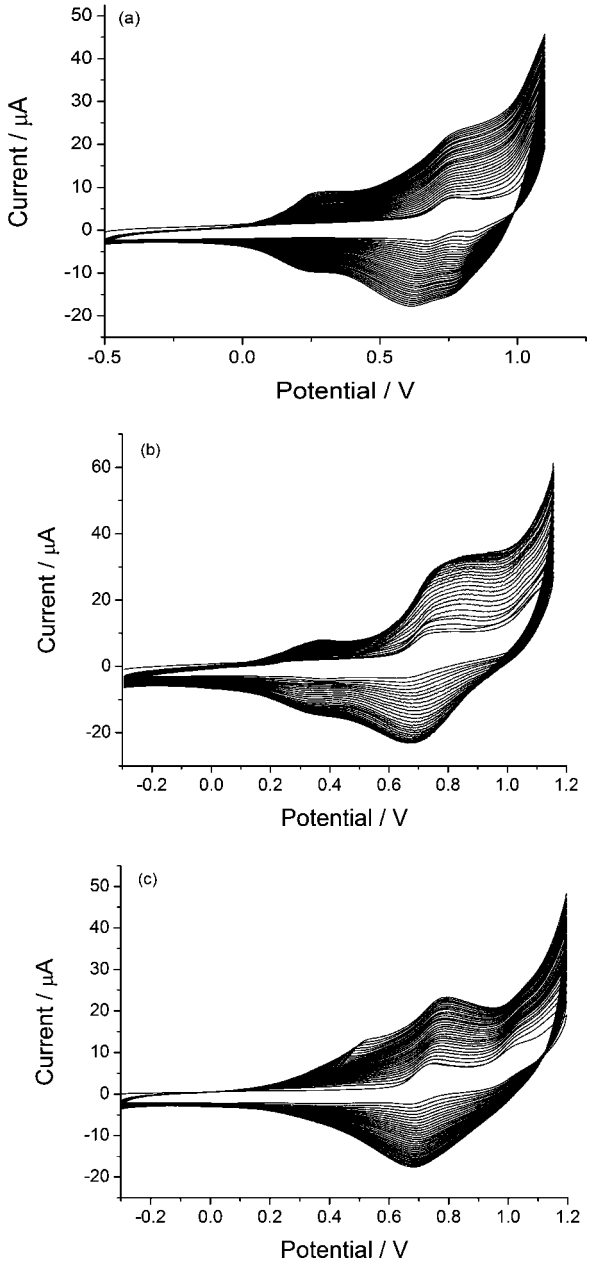

Figure 4. Electrochemical growth of (a) poly**1**, (b) poly**2**, and (c) poly**3** by cyclic voltammetry in CH_2Cl_2 using a carbon working electrode, Ag wire pseudoreference electrode, $(TBA)PF_6$ as the supporting electrolyte (0.1 M), substrate concentration 10^{-4} M, and scan rate 100 mV/s. The data are referenced to the Fc/Fc^+ redox couple.

dihydro−dithiin is 30.8°; these values are in good agreement with the crystal structure data.

According to the HOMO and HOMO-1 plots of all three compounds (Supporting Information), the removal of the first electron from each molecule originates from different sites. In compound **1**, the TTN unit is a better electron donor than the terthiophene fragment, and this is similar to the redox behavior of a closely related TTF−terthiophene-fused analogue (vide infra).[25] In **2**, the outer vinylene unit is reduced to a saturated bridge between the corresponding sulfur atoms, and the result is that the electron-donating property of the dihydro-TTN is decreased to the extent that the HOMO is spread over both types of sulfur heterocycles (dithiin and thiophene). For compound **3**, the dithiin ring holds little electron density, and the HOMO is dominant over the terthiophene chain. From the CV data, we observe that the difference between the two oxidation processes is ca. 0.35 to 0.40 V. From the computational data, the HOMO

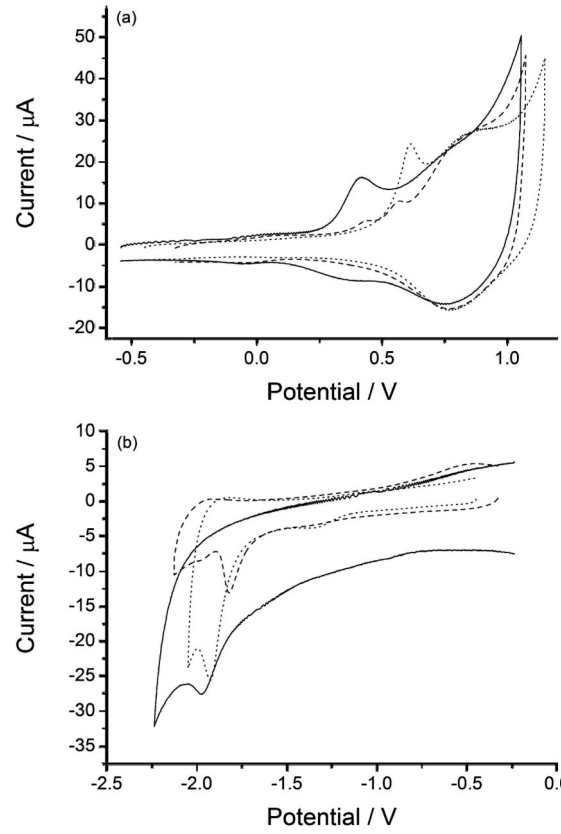

Figure 5. Cyclic voltammograms for (a) oxidation and (b) reduction of poly**1** (—), poly**2** (---), and poly**3** (•••) as films on a carbon working electrode. Experiments were conducted in monomer-free acetonitrile solution under the same conditions as those in Figure 4. The data are referenced to the Fc/Fc^+ redox couple.

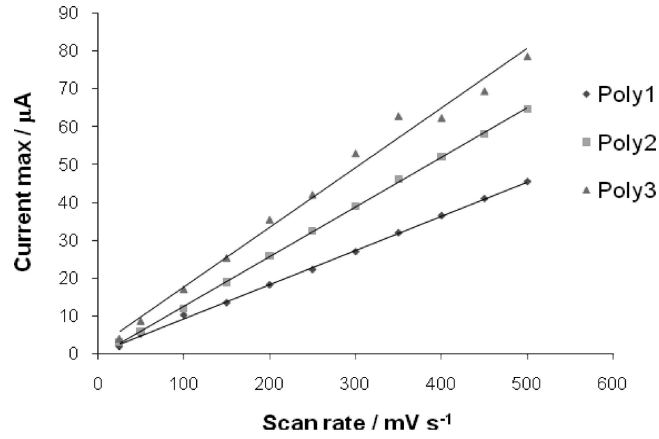

Figure 6. Plot of current versus scan rate for polymers.

Table 2. Electrochemical and Absorption Spectroscopy Data for Thin Films of Poly1, Poly2, and Poly3[a]

	E_{1ox}/V	E_{2ox}/V	E_{1red}/V	HOMO/eV	LUMO/eV	E_g/eV	λ_{max}/nm
Poly**1**	+0.42	+0.77	−1.97	−5.05	−3.01	2.04	436
Poly**2**	+0.56	+0.80	−1.82	−5.21	−3.14	2.07	471
Poly**3**	+0.60	+0.83	−1.93	−5.30	−3.19	2.11	450

[a] Experimental conditions are the same as those given in Figures 5 and 6. [b] HOMO and LUMO values are calculated from the onset of the first peak of the corresponding redox wave and referenced to ferrocene, which has a HOMO of −4.8 eV.

and HOMO-1 orbitals are close-lying with differences in the range 0.1 to 0.2 eV. Although the latter cannot be compared directly to the CV data (because there are charges involved in the latter), the HOMO-1 orbitals give some indication for the

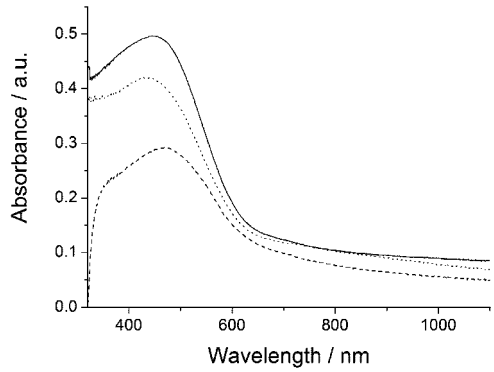

Figure 7. Electronic absorption spectra of poly**1** (—), poly**2** (---), and poly**3** (•••). Spectra were recorded on thin films deposited on ITO glass.

sites of the second oxidation process. For compounds **2** and **3**, the first oxidation already involves the terthiophene unit, indicating that polymerization can proceed from the cation radical species. Examination of the SOMO of the radical cation of **1** reveals that electron density is localized within the TTN unit. (See the Supporting Information.) Removal of a second electron to give the triplet diradical results in the spin density residing within the terthiophene unit. From these calculations, it is evident that the dication state must be reached to achieve polymerization of **1**. The following section describes the electropolymerization of compounds **1**−**3**.

Electrochemical Polymerization. The three monomer systems were polymerized electrochemically by repetitive cycling over both redox-active peaks. All three monomers polymerized readily, and the growth traces for the corresponding polymers are displayed in Figure 4. The electrochemistry of the three polymers was investigated in monomer-free acetonitrile with the same concentration of supporting electrolyte as before; the cyclic voltammograms of poly**1**, poly**2**, and poly**3** are shown in Figure 5. Prior to experiments, each polymer was dedoped to the neutral state by repetitive cycling in a region of no electroactivity (typically −0.4 to +0.1 V). The oxidation of the three polymers is shown in Figure 5a; in each case, the polymers feature a quasi-reversible oxidation wave followed by a large, broad, reversible wave. It is unlikely that the first wave represents a localized oxidation of the dithiin side group of the polymer because this is a fresh peak that emerges during the growth of the polymer. The potentials at which this first oxidation occurs differ for each polymer, with poly**1** considerably lower than its analogues (+0.42 V compared with poly**2** at +0.56 V and poly**3** at +0.60 V). The difference in this electrochemical behavior can be attributed to two factors: (i) the electronic contribution of the side groups and (ii) the morphology of the polymer films and subsequent interchain interactions. The second oxidation peaks are larger and broader than the first, and the potentials are similar (E_{2ox} for poly**1**, poly **2**, and poly**3** is +0.77, +0.80, and +0.83 V, respectively.) In view of these results, it can be envisaged that the removal of the first electrons from the polymers involves the dithiinothiophene heterocycle, whereas the second wave arises from the oxidation of bithiophene units in the polymer chain. This assumption is corroborated by UV−vis spectroelectrochemical measurements (see below) because the emergence of main-chain polarons is observed only after reaching the second oxidation wave. Furthermore, the quasi-irreversible nature of the first oxidation wave could be due to persistent, stabilized conformers generated within the dithiin rings upon removal of an electron. This phenomenon has been demonstrated in a related derivative, in which the dithiin ring becomes stabilized by reaching an

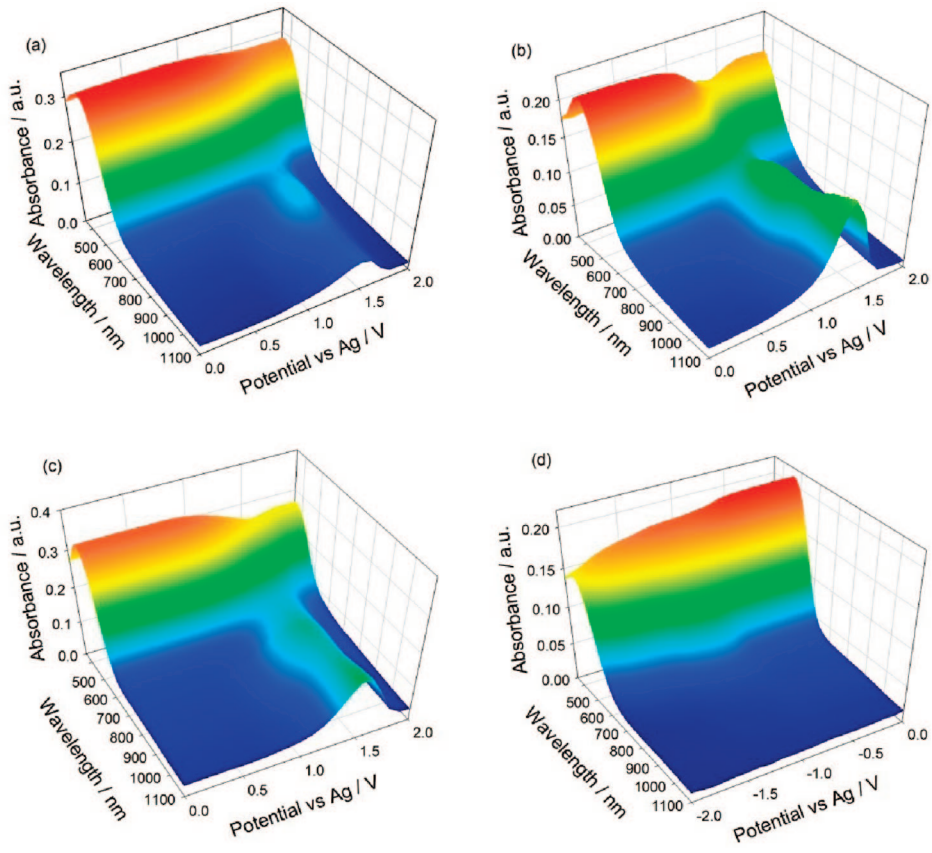

Figure 8. Absorption spectroelectrochemical plots of oxidation of (a) poly**1**, (b) poly**2**, and (c) poly**3** and reduction of (d) poly**3**. Potentials are given versus Ag wire pseudoreference electrode. The solvent was acetonitrile.

aromatic state upon oxidation.[31] For each of the polymers, a plot of scan rate versus current maximum for the first oxidation wave gives a linear fit (Figure 6), with R^2 values of 0.9991, 0.9996, and 0.9879 for poly**1**, poly**2**, and poly**3**, respectively. This confirms that charge transport through the polymer film is not diffusion limited.[50]

The reduction of the polymers is shown in Figure 5b. The irreversible reduction of poly**1** occurs at the most negative potential (−1.97 V), compared with the irreversible reductions of poly**2** (−1.82 V) and poly**3** (−1.93 V). Following the calculations for the terthiophene monomers, the electrons are added to the polythiophene chain, and the drop in potential (compared with that of the monomers) is due to the increased ability of the polymers to stabilize a negative polaron. For poly**1**, the small peak that is observed in its monomer would be hidden by the large peak at −1.97 V, so it is impossible to say if this additional reduction process exists in the polymer.

A useful analogy between **1**, poly**1**, and their TTF analogues can be made by considering the electrochemical properties of compound **8** and its polymer, the latter of which has been prepared from a chemical coupling route because compound **8** cannot be polymerized by oxidative coupling.[25] Referenced to ferrocene, **8** gives two reversible oxidation waves at $E^1_{1/2}$ = +0.24 V and $E^2_{1/2}$ = +0.62 V. The decrease in oxidation potentials compared with **1** shows that the TTF derivative is a better electron donor than the TTN analogue (**1**), and this reflects the difference between the electroactivity of the parent systems TTF and TTN, in which the former is more easily oxidized (TTF,[51] +0.34 and +0.71 V; TTN,[52] +0.69 and +1.16 V, vs SCE in acetonitrile solution). For poly**8**, the oxidation potentials are +0.29 and +0.67 V, which are higher than those of monomer **8** but still lower than those for poly**1** (by ca. 0.1 V). The electroactivity of poly**8** is complex, and the first oxidation is assigned to the TTF unit and the second to both TTF and polythiophene components.[25]

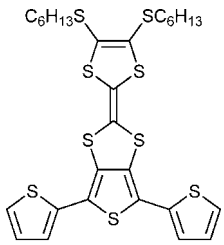

8

The electrochemical band gaps of poly**1**, poly**2**, and poly**3** were determined from the difference between the onsets of oxidation and reduction processes, which represent the HOMO and LUMO levels, respectively. To calculate the energy levels of these bands, the onsets were once again subtracted from the HOMO of ferrocene (−4.8 eV). A summary of these data can be seen in Table 2. The three polymers possess similar band gaps ranging from 2.04 to 2.11 eV, which are very similar to the optical band gap calculated for the polymers and to that of polythiophene itself.[53,54] This suggests that the side group has only little effect on conjugation. The optical band gap was calculated from the onset of the maximum absorption band of the three polymers (Figure 7) measured from films deposited on indium tin oxide (ITO) glass. The values calculated are 1.98, 1.98, and 2.00 eV for poly**1**, poly**2**, and poly**3**, respectively. The absorption maximum for poly**1** was found to be at 436 nm, which is shorter than that of poly**8** (λ_{max} = 496 nm, E_g = 1.82 eV, solid state).[25] This analogy demonstrates that a less-conjugated polymer is formed when the six-membered dithiin ring replaces the five-membered dithiole ring of poly**8**, possibly as a consequence of steric hindrance between thiophene sulfurs and the sulfurs of the larger dithiin unit.

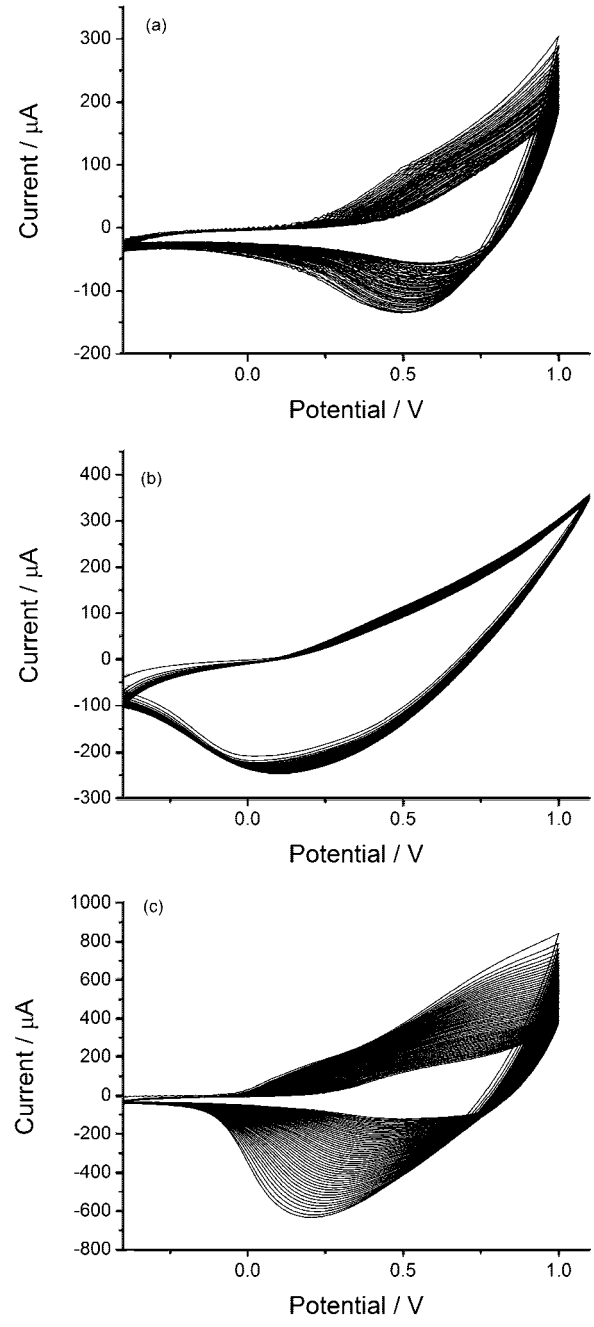

Figure 9. Stability of polymers (a) poly**1**, (b) poly**2**, and (c) poly**3** on ITO in monomer-free acetonitrile solution.

UV−vis spectroelectrochemical measurements were performed on films deposited on ITO glass over the oxidation range of all three polymers and then dedoped. Dedoping is used to expel trapped electrolyte by repetitive cycling in an electrochemical range where no activity takes place. The spectroelectrochemical plots of the oxidation of poly**1**, poly**2**, and poly**3** (Figure 8) all show similar p-doping. As mentioned above, there are no changes in the absorption spectra over the first oxidation waves, suggesting that the first electrons to be removed do not originate from the π-conjugated chain. New absorption waves form at +0.9 V in the wavelength region 600−800 nm and ca. 900 nm, attributed to the formation of positive polarons. Oxidation of the polymer chain leads to a disruption in the π-conjugated chain and hence a decrease in the absorbance of the $\pi-\pi^*$ band. For poly**1**, there is very little decrease in the

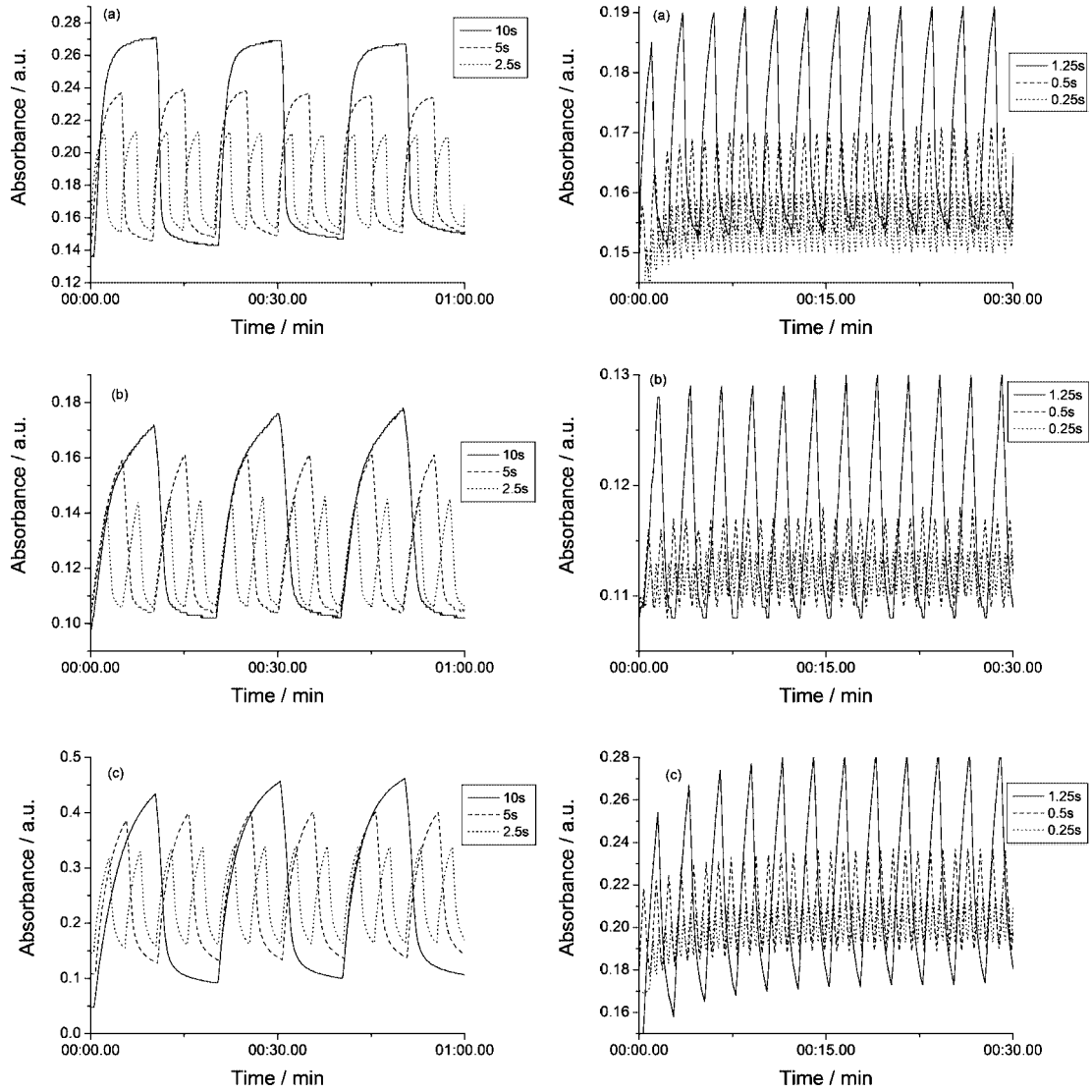

Figure 10. Change in absorbance upon p-doping at various switching rates for (a) poly**1**, (b) poly**2**, and (c) poly**3**. Absorbance was monitored at 755 nm between potentials of −0.4 and 1.5 V. The solvent was acetonitrile.

$\pi-\pi^*$ transition band (5% change in absorbance compared with 17 and 8% change for poly**2** and poly**3**), suggesting that oxidation involves the TTN side group instead of the polythiophene chain. This tends toward the effect seen with TTF attached to polythiophene in which the electroactivity is dominated by the TTF unit.[25,55] Reduction spectroelectrochemistry measurements were performed for the three polymers as well, but the only film that showed any significant change was poly**3** (Figure 8d), which gave a slight broadening of the absorbance in the range 600−800 nm between −0.8 and −1.2 V. There is also a decrease in the $\pi-\pi^*$ transition after −1.0 V, and these effects can be attributed to n-doping of the polythiophene chain.

We measured polymer stability for the three polymers on ITO (Figure 9) by subjecting the materials to repetitive oxidation cycles. It can be seen that poly**2** is the most stable toward p-doping with a decrease of only 17% in current response; poly**1** and poly**3** had decreases of 49 and 64%, respectively.

Polymer Switching. We measured the switching abilities of the three polymers by monitoring the absorbance of each polymer between two different potentials that will change the state from neutral to p-doped. The polymers were grown on ITO and dedoped. The potential was switched between −0.4 and 1.5 V, and the absorbance was measured at 755 nm, which provided the greatest change in absorbance. The switching times measured were 10, 5, 2.5, 1.25, 0.5, and 0.25 s. The changes in the absorbance can be seen in Figure 10 and are summarized in Table 3. Comparison of the percentage change in absorbance for the three polymers shows that poly**3** gives the greatest change; this is not unexpected because more open polymers give faster switching times because a less-packed morphology allows an efficient flow of counterions into and out of the polymer film.[40]

Table 3. Switching Times and Percentage Change in Absorbance

switching time (s)	% change poly**1**	% change poly**2**	% change poly**3**
10	45.9	42.7	79.8
5	36.1	35.4	66.2
2.5	28.2	26.9	51.6
1.25	18.9	16.9	39.3
0.5	10.0	6.8	19.0
0.25	6.3	3.5	9.3

Colorimetry. The CIE color coordinates of the polymers were measured for the neutral and doped states as the 1931 (*Yxy*) and 1976 ($L^*a^*b^*$) CIE representation of color space to determine the color transformation. *Y* is the luminance of the color with *x* and *y* coordinates of the chromaticity diagram.[56] L^* is lightness of the material with a^* and b^* opponent

Table 4. CIE *Yxy* and *L*a*b Color Spaces for Poly1, Poly2, and Poly3 for Neutral and Doped Polymers**

	Y	*x*	*y*	*L*	*a**	*b**
poly**1** neutral	47.67	0.3393	0.3313	74.62	6.74	7.87
poly**1** doped	52.72	0.3296	0.3358	77.71	1.21	8.04
poly**2** neutral	81.09	0.3212	0.3226	92.17	3.58	3.13
poly**2** doped	90.22	0.3178	0.3271	96.09	−0.22	4.27
poly**3** neutral	117.44	0.3145	0.3173	106.38	3.3	0.05
poly**3** doped	122.93	0.3131	0.3223	108.26	−0.28	1.87

dimensions of color. A positive *a** is red and a negative *a** is green. A positive *b** is yellow and a negative *b** is blue.[57] For all three of the polymers, the color changes from red (neutral) to yellow (doped). A summary of the color coordinates is shown in Table 4. Of the three polymers, poly**3** gives the greatest color contrast.

Conclusions

Three new monomers and their respective polymers have been synthesized and characterized by absorption spectroscopy, CV, UV−vis spectroelectrochemistry, electrochromic switching times, and colorimetry. The first monomer (**1**) has a fused TTN side group, which is an isomer of TTF. The other two monomers are the saturated (**2**) and open cycle form (**3**). Despite the similarity in structure to TTF, monomer **1** does not show any similar electrochemistry traits, such as the famous TTF two-wave oxidation or the formation of a new band at 390 nm in spectroelectrochemistry measurements upon p-doping. All three monomers show differences in oxidation and reduction potentials as well as band gap calculations; these effects have been explained in relation to structure comparisons. All three polymers showed electrochromic behavior with a visible color change from red to yellow with p-doping of the polymers. Poly**3** showed the best color contrast between neutral and oxidized states but was the least stable toward repetitive oxidation cycles.

Experimental Section

General. Melting points were taken using a Stuart Scientific SMP1 Melting Point apparatus and are uncorrected. ^{1}H and ^{13}C NMR spectra were recorded on a Bruker Avance/DPX400 apparatus at 400.13 and 100.61 MHz in $CDCl_3$. Chemical shifts are given in ppm; all *J* values are in Hz. Elemental analyses were obtained on a Perkin-Elmer 2400 analyzer. Electron absorption spectra were measured on a Unicam UV 300 spectrophotometer. MS LDI-TOF spectra were run on a Shimadzu Axima-CFR spectrometer (mass range 1−150 000 Da).

Electrochemistry. CV measurements were performed on a CH Instruments 660A electrochemical workstation with *iR* compensation using anhydrous dichloromethane or acetonitrile as the solvent. The electrodes were glassy carbon, platinum wire, and silver wire as the working, counter, and reference electrodes, respectively. All solutions were degassed (Ar) and contained monomer substrates in concentrations ca. 10^{-4} M, together with *n*-Bu_4NPF_6 (0.1 M) as the supporting electrolyte. All measurements are referenced against the $E^{1/2}$ of the Fc/Fc^+ redox couple. Spectroelectrochemical and switching experiments were conducted on ITO glass. Absorption spectra and CIE coordinates were recorded on a UNICAM UV 300 instrument.

1,3-Di(thiophene-2-yl)-2,4,5,8,9-pentathia-cyclopenta[*b*]-naphthalene (1). To an ice-cold solution of 2,3-bis(2-cyanoethyl-thio)-5,7-di(thiophen-2-yl)thieno[3,4-*b*][1,4]dithiin (**7**) (167 mg, 330 μmol) in THF, a solution of tetrabutylammonium hydroxide in methanol (1 M, 0.67 mL) was added dropwise, and the mixture was stirred for 1 h to form the corresponding 5,7-di(thiophen-2-yl)thieno[3,4-*b*][1,4]dithiine-2,3-dithiolate. *cis*-1,2-Dichloroethylene (28 μL, 360 μmol) was added, and the mixture was allowed to reach room temperature and was stirred for 3 days. The reaction was poured into 150 mL of NH_4Cl saturated solution. The precipitate formed was filtered and, after drying, dissolved in CS_2 and filtered through a plug of silica. After evaporation of the solvent, the crude product was recrystallized from CS_2/hexane to afford 128 mg (301 μmol, 92%) of yellow needles; mp 210−212 °C. Expected for $C_{16}H_8S_7$: C, 45.25; H, 1.90; S, 52.85. Found: C, 45.22; H, 2.13; S, 52.66. MS LDI-TOF +: 423.79 (M^+). MS LDI-TOF −: 397.95 ($(M-C_2H_2)^-$), 423.96 (M^-). ^{1}H NMR ($CDCl_3$, δ): 7.38 (dd, 2H, ^3J = 5.1 Hz, ^4J = 1.1 Hz), 7.25 (dd, 2H, ^3J = 3.7 Hz, ^4J = 1.2 Hz), 7.09 (dd, 2H, ^3J = 5.1 Hz, ^3J = 3.7 Hz), 6.49 (s, 4H). ^{13}C NMR ($CDCl_3$, δ): 133.6, 129.1, 128.4, 127.9, 127.2, 127.0, 126.6, 122.6.

1,3-Di(thiophene-2-yl)-6,7-dihydro-2,4,5,8,9-pentathiacyclo-penta[*b*]naphthalene (2). A freshly prepared solution of sodium methoxide (1.55 M, 0.32 mL) was added dropwise to an ice-cooled mixture of 5,7-di(thiophen-2-yl)-[1,3]dithiolo[4,5-*e*]thieno[3,4-*b*][1,4]dithiin-2-one (**5**) (100 mg, 234 μmol) in 10 mL of THF, and the mixture was stirred for 0.5 h. 1,2-Dibromoethane was added (22 μL, 253 μmol), and the mixture was stirred for 0.5 h. The reaction was allowed to reach room temperature, stirred overnight, and then subjected to MW heating for 1 h at 120 °C. After cooling, the solvent was removed under reduced pressure. The residue was dissolved in chloroform, filtered, and, after removal of the solvent, subjected to column chromatography on silica gel with DCM/petroleum ether (1:5) as the eluent. The main fraction was recrystallized from DCM/hexane to afford 65 mg (154 μmol, 65%) of yellow solid; mp 200−202 °C. Expected for $C_{16}H_{10}S_7$: C, 45.04; H, 2.36; S, 52.60. Found: C, 45.03; H, 2.34; S, 52.59. MS LDI-TOF +: 425.83 (M^+). MS LDI-TOF −: 397.95 ($(M-C_2H_4)^-$), 424.99 ($(M-H)^-$). ^{1}H NMR ($CDCl_3$, δ): 7.36 (dd, 2H, ^3J = 5.1 Hz, ^4J = 1.1 Hz), 7.29 (dd, 2H, ^3J = 3.7 Hz, ^4J = 1.1 Hz), 7.08 (dd, 2H, ^3J = 5.1 Hz, ^3J = 3.7 Hz), 3.27 (s, 4H). ^{13}C NMR ($CDCl_3$, δ): 134.0, 130.1, 128.7, 127.8, 126.8, 126.7, 121.9, 32.0.

2,3-Bis(methylthio)-5,7-di(thiophen-2-yl)thieno[3,4-*b*][1,4]-dithiin (3). A freshly prepared solution of sodium methoxide (0.64 M, 0.6 mL) was added dropwise to an ice-cooled mixture of 5,7-di(thiophen-2-yl)-[1,3]dithiolo[4,5-*e*]thieno[3,4-*b*][1,4]dithiin-2-one (**5**) (73 mg, 171 μmol) in 10 mL of THF, and the mixture was stirred for 0.5 h. Iodomethane (25 μL, 0.4 mmol) was added. The mixture was allowed to reach room temperature and was stirred overnight. The solvent was removed under reduced pressure. The residue was dissolved in chloroform, filtered and, after removal of the solvent, subjected to column chromatography on silica gel using DCM/petroleum ether (1:5) as the eluent. The main fraction was recrystallized from acetonitrile to afford 66 mg (154 μmol, 90%) of yellow plates; mp 122−124 °C. Expected for $C_{16}H_{12}S_7$: C, 44.83; H, 2.82; S, 52.35. Found: C, 44.84; H, 2.72; S, 52.11. MS APCI 429 ($(M+H)^+$). ^{1}H NMR ($CDCl_3$, δ): 7.37 (dd, 2H, ^3J = 5.1 Hz, ^4J = 1.1 Hz), 7.29 (dd, 2H, ^3J = 3.7 Hz, ^4J = 1.1 Hz), 7.08 (dd, 2H, ^3J = 5.1 Hz, ^3J = 3.7 Hz), 2.49 (s, 6H). ^{13}C NMR ($CDCl_3$, δ): 134.2, 131.5, 129.7, 128.5, 127.6, 126.7, 126.6, 18.9.

5,6-Bis(2-thienoyl)-5,6-dihydro-[1,3]dithiolo[4,5-*b*][1,4]-dithiin-2-one (4b). A mixture of 5,6-bis(2-thienoyl)-5,6-dihydro-[1,3]dithiolo[4,5-*b*][1,4]dithiin-2-thione (**4a**) (2.14 g, 4.82 mmol), mercury acetate (2.55 g), acetic acid (90 mL), and dichloromethane (270 mL) was stirred for 16 h. The precipitate was filtered off and rinsed with dichloromethane. The combined filtrates were washed with water, sodium hydrogen carbonate, and water again. Drying with magnesium sulfate and evaporation of the solvent afforded 1.86 g (4.33 mmol, 90%) of the yellow solid; mp 180−184 °C. Expected for $C_{15}H_8O_3S_6$: C, 42.03; H, 1.88; S, 44.89. Found: C, 41.68; H, 1.70; S, 44.60. MS LDI-TOF −: 426.87 ($(M-H)^-$). ^{1}H NMR ($CDCl_3$, δ): 7.92 (dd, 2H, ^3J = 3.9 Hz, ^4J = 1.1 Hz), 7.78 (dd, 2H, ^3J = 4.9 Hz, ^4J = 1.1 Hz), 7.21 (dd, 2H, ^3J = 4.9 Hz, ^3J = 3.9 Hz), 5.56 (s, 2H). ^{13}C NMR ($CDCl_3$, δ): 188.5, 184.3, 140.7, 136.1, 134.1, 128.5, 123.8, 54.4.

5,7-Di(thiophen-2-yl)-[1,3]dithiolo[4,5-*e*]thieno[3,4-*b*][1,4]-dithiin-2-one (5). A mixture of 5,6-bis(2-thienoyl)-5,6-dihydro-[1,3]dithiolo[4,5-*b*][1,4]dithiin-2-one (**4b**) (1.41 mg, 3.28 mmol), phosphorus pentasulfide (6.97 g), and $NaHCO_3$ (2.25 g) in 70 mL of dioxane was stirred at 90 °C for 2 h. After cooling, water (150 mL) was added to destroy excess phosphorus pentasulfide, and the mixture was stirred at 70 °C for 1 h. After the mixture was poured into 200 g of ice water, the precipitate was filtered off and washed

with water. The crude product was dried, dissolved in hot toluene, and filtered through a plug of silica. After the solution was concentrated under reduced pressure, the filtrate was cooled down, and the product was filtered off and washed with cold toluene to provide 1.17 g (2.74 mmol, 84%) of light-yellow powder; mp 260−264 °C. Expected for $C_{15}H_6OS_7$: C, 42.23; H, 1.42; S, 52.61. Found: C, 42.18; H, 1.34; S, 52.64. MS LDI-TOF +: 425.68 (M^+). ^{1}H NMR ($CDCl_3$, δ): 7.42 (dd, 2H, ^3J = 5.1 Hz, ^4J = 1.0 Hz), 7.28 (dd, 2H, ^3J = 3.6 Hz, ^4J = 1.0 Hz), 7.12 (dd, 2H, ^3J = 5.1 Hz, ^3J = 3.7 Hz).

2,3-Bis(2-cyanoethylthio)-5,7-di(thiophen-2-yl)thieno[3,4-*b*]-[1,4]dithiin (7). To an ice-cold mixture of 5,7-di(thiophen-2-yl)-[1,3]dithiolo[4,5-*e*]thieno[3,4-*b*][1,4]dithiin-2-one (**5**) (215 mg, 504 μmol) in THF was added sodium methoxide (25%, 4.37 M, 0.36 mL) dropwise, and the mixture was stirred for 0.5 h. 3-Bromopropionitrile (0.24 mL, 2.9 mmol) was added. The mixture was allowed to reach room temperature and was stirred overnight. The solvent was removed under reduced pressure, and the residue was dissolved in chloroform, filtered and, after removal of the solvent, subjected to column chromatography on silica gel using DCM as the eluent. The main fraction (240 mg) was recrystallized from toluene to afford 202 mg (79%) of yellow needles; mp 164−165 °C. Expected for $C_{20}H_{14}N_2S_7$: C, 47.40; H, 2.78; S, 44.29. Found: C, 47.58; H, 2.87; N, 5.22; S, 44.28%. MS LDI-TOF +: 505.73 (M^+). ^{1}H NMR ($CDCl_3$, δ): 7.42 (dd, 2H, ^3J = 5.1 Hz, ^4J = 1.1 Hz), 7.29 (dd, 2H, ^3J = 3.7 Hz, ^4J = 1.1 Hz), 7.10 (dd, 2H, ^3J = 5.1 Hz, ^3J = 3.7 Hz), 3.26 (t, 4H, ^3J = 7.0 Hz), 2.56 (t, 4H, ^3J = 7.0 Hz). ^{13}C NMR ($CDCl_3$, δ): 133.5, 132.2, 129.8, 128.5, 127.9, 127.2, 127.1, 117.7, 30.5, 19.0.

X-ray Crystallography. The weakly scattering small crystals of **1** required synchrotron radiation for successful study (Daresbury SRS station 9.8, Bruker APEXII diffractometer), which was also hampered by crystal twinning, leading to relatively high *R* factors, generally low precision, and some residual electron density peaks; however, there is no apparent disorder, and the conformations of the two crystallographically independent molecules in the asymmetric unit are clear. Compound **2** was investigated using a Bruker-Nonius KappaCCD diffractometer and rotating-anode Mo Kα radiation; this structure is also fully ordered. Details of crystallographic data and results are in the Supporting Information.

Acknowledgment. We thank the EPSRC for a research grant to A.L.K. (GR/T28379) and for funding the U.K. National Crystallography Service. We also thank the STFC for access to synchrotron facilities.

Supporting Information Available: X-ray crystal packing diagrams, HOMO, HOMO-1, LUMO, and SOMO plots, tables of bond lengths, angles, and experimental data, and details of crystallographic data and results. This material is available free of charge via the Internet at http://pubs.acs.org.

References and Notes

(1) Chiang, C. K.; Fincher, C. R.; Park, Y. W.; Heeger, A. J.; Shirakawa, H.; Louis, E. J.; Gau, S. C.; Macdiarmid, A. G. *Phys. Rev. Lett.* **1977**, *39*, 1098–1101.
(2) Higgins, S. J. *Chem. Soc. Rev.* **1997**, *26*, 247–257.
(3) Schwendeman, I.; Hwang, J.; Welsh, D. M.; Tanner, D. B.; Reynolds, J. R. *Adv. Mater.* **2001**, *13*, 634–637.
(4) Cirpan, A.; Argun, A. A.; Grenier, C. R. G.; Reeves, B. D.; Reynolds, J. R. *J. Mater. Chem.* **2003**, *13*, 2422–2428.
(5) Sonmez, G.; Sonmez, H. B.; Shen, C. K. F.; Jost, R. W.; Rubin, Y.; Wudl, F. *Macromolecules* **2005**, *38*, 669–675.
(6) Kraft, A.; Grimsdale, A. C.; Holmes, A. B. *Angew. Chem., Int. Ed.* **1998**, *37*, 402–428.
(7) Elschner, A.; Heuer, H. W.; Jonas, F.; Kirchmeyer, S.; Wehrmann, R.; Wussow, K. *Adv. Mater.* **2001**, *13*, 1811–1814.
(8) Mitschke, U.; Bauerle, P. *J. Mater. Chem.* **2000**, *10*, 1471–1507.
(9) Forrest, S. R. *Nature* **2004**, *428*, 911–918.
(10) Dimitrakopoulos, C. D.; Malenfant, P. R. L. *Adv. Mater.* **2002**, *14*, 99+.
(11) Horowitz, G. *Adv. Mater.* **1998**, *10*, 365–377.
(12) Bao, Z. N.; Rogers, J. A.; Katz, H. E. *J. Mater. Chem.* **1999**, *9*, 1895–1904.
(13) Ling, M. M.; Bao, Z. N. *Chem. Mater.* **2004**, *16*, 4824–4840.
(14) Brabec, C. J.; Sariciftci, N. S.; Hummelen, J. C. *Adv. Funct. Mater.* **2001**, *11*, 15–26.
(15) Segura, J. L.; Martin, N.; Guldi, D. M. *Chem. Soc. Rev.* **2005**, *34*, 31–47.
(16) Cravino, A.; Sariciftci, N. S. *J. Mater. Chem.* **2002**, *12*, 1931–1943.
(17) Koezuka, H.; Tsumura, A.; Ando, T. *Synth. Met.* **1987**, *18*, 699–704.
(18) Goldenberg, L. M.; Skabara, P. J.; Roberts, D. M.; Berridge, R.; Ortí, E.; Viruela, P. M.; Pou-Amérigo, R. *J. Mater. Chem.* **2000**, *10*, 2458–2465.
(19) Swager, T. M.; Marsella, M. J. *Adv. Mater.* **1994**, *6*, 595–597.
(20) McQuade, D. T.; Pullen, A. E.; Swager, T. M. *Chem. Rev.* **2000**, *100*, 2537–2574.
(21) Albert, K. J.; Lewis, N. S.; Schauer, C. L.; Sotzing, G. A.; Stitzel, S. E.; Vaid, T. P.; Walt, D. R. *Chem. Rev.* **2000**, *100*, 2595–2626.
(22) Segura, J. L.; Martin, N. *Angew. Chem., Int. Ed.* **2001**, *40*, 1372–1409.
(23) Ferraris, J.; Cowan, D. O.; Walataka, V., Jr.; Perlstein, J. H. *J. Am. Chem. Soc.* **1973**, *95*, 948–949.
(24) Frère, P.; Skabara, P. J. *Chem. Soc. Rev.* **2005**, *34*, 69–98.
(25) Berridge, R.; Skabara, P. J.; Pozo-Gonzalo, C.; Kanibolotsky, A.; Lohr, J.; McDouall, J. J. W.; McInnes, E. J. L.; Wolowska, J.; Winder, C.; Sariciftci, N. S.; Harrington, R. W.; Clegg, W. *J. Phys. Chem. B* **2006**, *110*, 3140–3152.
(26) Thobiegautier, C.; Gorgues, A.; Jubault, M.; Roncali, J. *Macromolecules* **1993**, *26*, 4094–4099.
(27) Huchet, L.; Akoudad, S.; Roncali, J. *Adv. Mater.* **1998**, *10*, 541–545.
(28) Garin, J.; Andreu, R.; Orduna, J.; Royo, J. M. *Synth. Met.* **2001**, *120*, 749–750.
(29) Wang, C. G.; Benz, M. E.; Legoff, E.; Schindler, J. L.; Allbrittonthomas, J.; Kannewurf, C. R.; Kanatzidis, M. G. *Chem. Mater.* **1994**, *6*, 401–411.
(30) Gurunathan, K.; Murugan, A. V.; Marimuthu, R.; Mulik, U. P.; Amalnerkar, D. P. *Mater. Chem. Phys.* **1999**, *61*, 173–191.
(31) Skabara, P. J.; Berridge, R.; Prescott, K.; Goldenberg, L. M.; Ortí, E.; Viruela, R.; Pou-AméRigo, R.; Batsanov, A. S.; Howard, J. A. K.; Coles, S. J.; Hursthouse, M. B. *J. Mater. Chem.* **2000**, *10*, 2448–2457.
(32) Seong, S.; Marynick, D. S. *J. Phys. Chem.* **1994**, *98*, 13334–13338.
(33) Kobayashi, K.; Gajurel, C. L. *Sulfur Rep.* **1986**, *7*, 123–52.
(34) Moses, P. R.; Harnden, R. M.; Chambers, J. Q. *J. Electroanal. Chem.* **1977**, *84*, 187–194.
(35) Harnden, R. M.; Moses, P. R.; Chambers, J. Q. *J. Chem. Soc., Chem. Commun.* **1977**, 11–12.
(36) Sugimoto, T.; Sugimoto, I.; Kawashima, A.; Yamamoto, Y.; Misaki, Y.; Yoshida, Z. *Heterocycles* **1987**, *25*, 83–88.
(37) Roncali, J. *Chem. Rev.* **1992**, *92*, 711–738.
(38) Doi, S.; Kuwabara, M.; Noguchi, T.; Ohnishi, T. *Synth. Met.* **1993**, *57*, 4174–4179.
(39) Sapp, S. A.; Sotzing, G. A.; Reynolds, J. R. *Chem. Mater.* **1998**, *10*, 2101–2108.
(40) Argun, A. A.; Aubert, P. H.; Thompson, B. C.; Schwendeman, I.; Gaupp, C. L.; Hwang, J.; Pinto, N. J.; Tanner, D. B.; MacDiarmid, A. G.; Reynolds, J. R. *Chem. Mater.* **2004**, *16*, 4401–4412.
(41) Sonmez, G.; Sonmez, H. B.; Shen, C. K. E.; Wudl, F. *Adv. Mater.* **2004**, *16*, 1905-+.
(42) Sonmez, G.; Wudl, F. *J. Mater. Chem.* **2005**, *15*, 20–22.
(43) Skabara, P. J.; Serebryakov, I. M.; Roberts, D. M.; Perepichka, I. F.; Coles, S. J.; Hursthouse, M. B. *J. Org. Chem.* **1999**, *64*, 6418–6424.
(44) Chung, T. C.; Kaufman, J. H.; Heeger, A. J.; Wudl, F. *Phys. Rev. B* **1984**, *30*, 702–710.
(45) Pozo-Gonzalo, C.; Berridge, R.; Skabara, P. J.; Cerrada, E.; Laguna, M.; Coles, S. J.; Hursthouse, M. B. *Chem. Commun.* **2002**, 2408–2409.
(46) Skabara, P. J.; Pozo-Gonzalo, C.; Miazza, N. L.; Laguna, M.; Cerrada, E.; Luquin, A.; González, B.; Coles, S. J.; Hursthouse, M. B.; Harrington, R. W.; Clegg, W. *Dalton Trans.* **2008**, 3070–3079.
(47) Berridge, R.; Wright, S. P.; Skabara, P. J.; Dyer, A.; Steckler, T.; Argun, A. A.; Reynolds, J. R.; Ross, W. H.; Clegg, W. *J. Mater. Chem.* **2007**, *17*, 225–231.
(48) Spencer, H. J.; Skabara, P. J.; Giles, M.; McCulloch, I.; Coles, S. J.; Hursthouse, M. B. *J. Mater. Chem.* **2005**, *15*, 4783–4792.
(49) Pozo-Gonzalo, C.; Khan, T.; McDouall, J. J. W.; Skabara, P. J.; Roberts, D. M.; Light, M. E.; Coles, S. J.; Hursthouse, M. B.; Neugebauer, H.; Cravino, A.; Sariciftci, N. S. *J. Mater. Chem.* **2002**, *12*, 500–510.
(50) Lyons, M. E. G. *Charge Percolation in Electroactive Polymers in Electroactive Polymer Chemistry, Part 1: Fundamentals*; Plenum Press: New York, 1994.
(51) Green, D. C. *J. Org. Chem.* **1979**, *44*, 1476–1479.
(52) Schroth, W.; Borsdorf, R.; Herzschu., R.; Seidler, J. *Z. Chem.* **1970**, *10*, 147–148.

(53) Chandrasekhar, P. *Conducting Polymers, Fundamentals and Applications: A Practical Approach*; Kluwer Academic: Dordrecht, 1999.
(54) Pei, Q. B.; Zuccarello, G.; Ahlskog, M.; Inganas, O. *Polymer* **1994**, *35*, 1347–1351.
(55) Skabara, P. J.; Berridge, R.; McInnes, E. J. L.; West, D. P.; Coles, S. J.; Hursthouse, M. B.; Müllen, K. *J. Mater. Chem.* **2004**, *14*, 1964–1969.
(56) Thompson, B. C.; Schottland, P.; Zong, K. W.; Reynolds, J. R. *Chem. Mater.* **2000**, *12*, 1563–1571.
(57) Rauh, R. D.; Wang, F.; Reynolds, J. R.; Meeker, D. L. *Electrochim. Acta* **2001**, *46*, 2023–2029.

MA900010N